

## Research Article

# Insulin-Loaded pH-Sensitive Hyaluronic Acid Nanoparticles Enhance Transcellular Delivery

Lina Han,<sup>1,2</sup> Yuefang Zhao,<sup>1,2</sup> Lifang Yin,<sup>1,2</sup> Ruiming Li,<sup>3</sup> Yang Liang,<sup>1,2</sup> Huan Huang,<sup>1,2</sup> Shirong Pan,<sup>3</sup> Chuanbin Wu,<sup>1,2</sup> and Min Feng<sup>1,2,4</sup>

Received 29 February 2012; accepted 16 May 2012; published online 30 May 2012

**Abstract.** In the present study, we developed novel insulin-loaded hyaluronic acid (HA) nanoparticles for insulin delivery. The insulin-loaded HA nanoparticles were prepared by reverse-emulsion-freeze-drying method. This method led to a homogenous population of small HA nanoparticles with average size of 182.2 nm and achieved high insulin entrapment efficiencies (approximately 95%). The pH-sensitive HA nanoparticles as an oral delivery carrier showed advantages in protecting insulin against the strongly acidic environment of the stomach, and not destroying the junction integrity of epithelial cells which promise long-term safety for chronic insulin treatment. The results of transport experiments suggested that insulin-loaded HA nanoparticles were transported across Caco-2 cell monolayers mainly *via* transcellular pathway and their apparent permeability coefficient from apical to basolateral had more than twofold increase compared with insulin solution. The efflux ratio of  $P_{app}$  (B to A) to  $P_{app}$  (A to B) less than 1 demonstrated that HA nanoparticle-mediated transport of insulin across Caco-2 cell monolayers underwent active transport. The results of permeability through the rat small intestine confirmed that HA nanoparticles significantly enhanced insulin transport through the duodenum and ileum. Diabetic rats treated with oral insulin-loaded HA nanoparticles also showed stronger hypoglycemic effects than insulin solution. Therefore, these HA nanoparticles could be a promising candidate for oral insulin delivery.

**KEY WORDS:** high entrapment efficiency; hyaluronic acid nanoparticles; insulin; pH sensitive; transcellular delivery.

## INTRODUCTION

The discovery of insulin was one of the greatest medical advances of the last century. It has saved countless lives of people with insulin-dependent diabetes mellitus. Oral administration is the desirable route for insulin delivery, as it can take advantage of the portal-hepatic route of absorption to directly inhibit hepatic glucose production as well as improve patient compliance. However, oral administration of insulin was found to be ineffective for the treatment of insulin-dependent diabetes mellitus, as insulin has low permeability across the intestinal epithelium and is strongly degraded by proteolytic enzymes in the gastrointestinal tract, resulting in insufficient bioavailability (1). Up to now, the subcutaneous route by injection remains the most effective and irreplaceable method

for insulin therapy, although it needs multiple daily injections often leading to poor patient compliance and may cause upsetting side effects such as hypoglycemia (2).

Insulin encapsulated in nanoparticles as one of many strategies has been developed to enhance the absorption and aims to achieve successful oral delivery of insulin. Various polymeric-based nanoparticle systems including chitosan/alginate (3), poly (lactic-co-glycolic acid) (PLGA) (4), and solid lipid nanoparticles (5) are widely investigated. Furthermore, the ligand-modified nanoparticles (such as avidin- and biotin-modified nanoparticles) have received much attention for their active intracellular transport (6). Previous studies have demonstrated that lectin and vitamin B<sub>12</sub> conjugated nanoparticles have shown to improve cellular uptake in absorptive enterocytes (7,8). Use of these nanotechnologies to orally deliver insulin have several advantages to overcome the barriers in gastrointestinal tract, such as protection of encapsulated insulin from enzymatic degradation by its entrapment in the nanoparticles (9), enhancement in insulin permeability across Caco-2 cell monolayers and improvement of oral absorption in diabetic animal models at various degrees (10). Despite these encouraging research results, however, till now, using any of these nanoparticle systems for oral insulin delivery has not yet been approved as available drug products. Major limitations of current insulin-loaded nanoparticles to be used in clinical practice are their low drug entrapment

<sup>1</sup> Department of Pharmacy, School of Pharmaceutical Sciences, Sun Yat-sen University, University Town, Guangzhou 510006, People's Republic of China.

<sup>2</sup> Research and Development Center of Pharmaceutics of Guangdong Province, University Town, Guangzhou 510006, People's Republic of China.

<sup>3</sup> The First Affiliated Hospital, Sun Yat-sen University, 80 Zhongshan Road II, Guangzhou 510080, People's Republic of China.

<sup>4</sup> To whom correspondence should be addressed. (e-mail: fengmin@mail.sysu.edu.cn)

efficiency, insufficient amounts of intestinal absorption and the potential toxicity problems owing to the continuous absorption of particles (11). Furthermore, the high cost of the nanoparticle-based formulation, in particular of ligand-conjugated nanoparticles, also is the key fact to restrict its widespread use for the daily administration of insulin for patients' entire lives (12).

Hyaluronic acid (HA) is a naturally occurring polyanionic biopolymer, composed of D-glucuronic acid and D-N-acetylglucosamine, linked *via* alternating  $\beta$ -1, 4 and  $\beta$ -1, 3 glycosidic bonds. It is one of the major components of the extracellular matrix of connective tissues and present in synovial fluid of joints, in the vitreous body, in umbilical cord, and in scaffolding that comprises cartilage. It plays an important role in many biological processes such as in tissue hydration, in organization of the extracellular matrix, in lubrication, and in wound healing (13,14). HA has been extensively investigated for several biomedical applications, such as tissue engineering and drug and gene delivery systems, because of its biocompatibility, biodegradability, and readily modified chemical structure (15).

The present work described the preparation and characterization of insulin-loaded HA nanoparticles with high drug entrapment efficiency. The HA nanoparticles as an oral delivery carrier protecting insulin against proteolytic enzymes and a strong-acidic gastric environment was investigated. The cellular uptake and permeability of insulin-loaded HA nanoparticles through Caco-2 cell monolayers and rat small intestine was specifically evaluated. Their pharmacological effect was also determined by measuring the decrease of plasma glucose levels in diabetic rats.

## MATERIALS AND METHODS

### Materials

Human insulin of recombinant DNA origin (100 IU/mL) was purchased from Xuzhou Wanbang Biochemical Pharmaceutical Co., China. Sodium hyaluronate ( $MW=1.0\times 10^6$  Da) was purchased from Shandong Freda Biopharm Co., Ltd. Adipic acid dihydrazide (ADH) and 1-[3-(dimethylamino)propyl]-3-ethylcarbodiimide hydrochloride (EDC·HCl) were from Aladdin Reagent Co. Dulbecco's Modified Eagle Media (DMEM), fetal calf serum, nonessential amino acids, phosphate-buffered saline (PBS), trypsin/EDTA solution (0.2% of EDTA and 0.25% of trypsin in PBS) and Hanks' balanced salt solution (HBSS) were purchased from Gibco-BRL Life Technologies. Caco-2 cells originating from a human colorectal carcinoma were obtained from American Type Culture Collection. Fluorescein isothiocyanate (FITC) and streptozotocin (STZ) were obtained from Sigma-Aldrich. All other reagents were of analytical grade.

### Differential Scanning Calorimetry

The interactions between hyaluronic acid and insulin were determined by differential scanning calorimetry (DSC; NETZSCH, STA 409PC), which was a measurement regarding transitions involving endothermic or exothermic processes. The operational conditions were as follows: heating rate 5°C/min, from 30°C to 270°C, flow rate of N<sub>2</sub> was 50 mL/min. An empty pan was used as reference.

### Preparation of Insulin-Loaded HA Nanoparticles by Reverse-Emulsion–Freeze-Drying Method

Insulin-loaded HA nanoparticles were prepared by two-step process using a modified reverse emulsion evaporation method. The first step was to prepare insulin-loaded HA nanoparticle-dispersed solution. Briefly, 20 mg of sodium hyaluronate (HA) and 5 mg of insulin was dissolved in 2 mL of double deionized water containing 2% (*w/v*) of Tween 80 while stirring to form the aqueous phase. Next, 0.80 mg of ADH (10:1 molar ratio of the carboxyl groups of HA to ADH) as cross-linker was added to HA solution. The pH of the reaction mixture was adjusted to 4.7 by the addition of 1 N HCl. After that, 0.9 mg of EDC (1:1 molar ratio of ADH to EDC) was added to the mixture. Then, the aqueous phase was added dropwise into the 8 mL of cyclohexane containing 2% (*w/v*) of Span 80 under mechanical stirring by a high-speed mixer at 10,000 rpm for 3 min. After this process, the cross-linking reaction between HA and ADH in reverse emulsion took another 2 h under continuous magnetic stirring at 100 rpm.

The second step was to collect insulin-loaded HA nanoparticle dry powder. The 2 mL of supersaturated solution of mannitol (at 30°C) containing 0.5% (*w/v*) of Tween 80 and 8 mL of cyclohexane containing 0.5% (*w/v*) of Span 80 were mixed, and then dispersed by high-speed mixer to obtain mannitol emulsion. The mannitol emulsion was poured into insulin-loaded HA nanoparticle emulsion and extensively mixed. The mixture was pre-frozen at  $-80^{\circ}\text{C}$  for 24 h and then lyophilized (LGJ-10 C, Xiangyi Co., China) below 20 Pa for 24 h.

### Particle Size, Zeta Potential, and Morphology

The particle size and Zeta potential measurements were carried out by photon correction spectroscopy and laser Doppler anemometry, respectively (Zetasizer Nano ZS90, Malvern Instruments Ltd., UK). Measurements were carried out at 25°C using ultrapure water as diluent to a proper concentration. Each batch was analyzed in triplicate.

The morphology of insulin-loaded HA nanoparticles was observed by transmission electron microscopy (TEM). For the TEM observations, a drop of nanoparticle suspension was placed on a 300-mesh formvar carbon-coated copper grid and allowed to equilibrate for 3 min. Solution was wiped off with filter paper and the grids were then stained with 2% phosphotungstic acid and allowed to air dry. Images were taken using a JEM-1400 TEM (JEOL, Japan) at 120 kV.

### Reversed Phase High-Performance Liquid Chromatography

Insulin concentrations in HA nanoparticles were determined by reversed phase high-performance liquid chromatography (RP-HPLC). HPLC analyses were performed with a Waters (Waters Corp., Milford, MA) 1525 binary pump equipped with a Waters 2487 Dual  $\lambda$  Absorbance Detector (set at the wavelength of 214 nm), an injection autosampler (Waters 717 plus) and processed by Breeze™ Software Build. The column (Gemini 5  $\mu\text{m}$  C18 110 Å, 250 $\times$ 4.60 mm, Phenomenex) was maintained at 40°C throughout the run. The mobile phase consisted of a mixture of phosphate buffer

(pH 3.0) and acetonitrile (73:27, v/v). The method had good linear relationship within the range of 5 to 100  $\mu\text{g/mL}$ , and the RSD of average recovery was lower than 2%. The resolution between two peaks in HPLC chromatograph was higher than 1.5, which ensured the complete separation of insulin and other components of HA nanoparticles.

### Insulin Entrapment Efficiency

To assay the insulin entrapment efficiency, 10 mg of insulin-loaded HA nanoparticle dry powder and 5 mL of phosphate buffer (pH 7.4) were mixed homogeneously. The mixture was stirred (100 rpm) at 4°C for 48 h, and then centrifuged at 16,000 $\times g$  for 60 min. Finally the supernatant was analyzed by RP-HPLC.

### Synthesis of FITC-Insulin

For the qualitative and quantitative analysis of insulin in Caco-2 cell monolayer transport studies, FITC-labeled insulin was synthesized. FITC-labeled insulin was synthesized based on the reaction between the isothiocyanate group of FITC and the amine groups of insulin, as previous described (16). Briefly, 5 mg of FITC was dissolved in 1 mL of DMSO and added dropwise to a 20 mL of sodium carbonate solution (0.1 M) containing 100 mg of insulin. Upon addition of FITC, the reaction vials were protected from light and allowed to mix under magnetic stirring for 12 h at 4°C. To quench the excess FITC, 7 mL of ammonium chloride solution (0.2 M) was added into the reaction vials under magnetic stirring for 2 h. The mixture was then purified by dialysis (3000 MWCO), and lyophilized to obtain the FITC-labeled insulin dry powder.

### In Vitro Release of Insulin Under Simulated Gastrointestinal Conditions

To determine insulin released from HA nanoparticles in enzyme-free simulated digestive fluids, 5 mg of insulin-loaded HA nanoparticles were incubated in 10 mL of simulated gastric fluid without enzyme (SGF) (USP-NF 26, pH 1.2) for 120 min; after decanting SGF, HA nanoparticles were immersed into simulated intestinal fluid without enzyme (SIF) (USP-NF26, pH 6.8) for another 180 min at 37°C under stirring (100 rpm). Sample solution (1 mL) were collected and replaced by the same volume of incubation medium at determined time intervals. For the quantitative analysis of insulin released from HA nanoparticles, samples were centrifuged at 18,000 $\times g$  for 30 min at 4°C, and 300  $\mu\text{L}$  of supernatant was analyzed by RP-HPLC. The release studies were carried out in triplicate.

### Proteolytic Studies

To assess the protective effect against gastric degradation, 5 mg of insulin-loaded HA nanoparticles was incubated at 37°C and shaken with 10 mL of pepsin solution (30 IU/ml, pH 1.2) for 2 h. The enzyme was dissolved in the gastric juice immediately before starting the experiment to prevent loss of activity. At scheduled times, 500  $\mu\text{L}$  of samples were taken out for testing. The pepsin digestion reaction was stopped by

adding NaOH solution (0.05 M). The concentrations of undegraded insulin in the samples were determined by RP-HPLC.

To assess the protective effect against intestinal degradation, 5 mg of insulin-loaded HA nanoparticles were added to trypsin solution (0.025% of trypsin in PBS, pH 7.4), and the trypsin digestion reaction was stopped by adding 0.1 M HCl solution. All other procedures were the same as the above pepsin experiment.

### Insulin Transport Study

Human colorectal carcinoma cells (Caco-2 cells) monolayer was chosen as an ideal drug transport cell model. Caco-2 cells of passage 40–70 were seeded at a density of  $2 \times 10^5$  cells/ $\text{cm}^2$  into separate chambers (Costar Transwell Plate, Corning and Life) and cultured for 21 days in 0.2 mL of supplemented DMEM in order to form a confluent monolayer. Medium was changed on alternate days in the first 7 days, and changed every day thereafter. After 21 days, the transendothelial electrical resistance (TEER) was measured with an EVOM volt-ohm meter and a chopstick electrode (World Precision Instruments, Sarasota, FL), only the wells with the TEER value higher than 400  $\Omega\text{cm}^2$  (after deducting the blank) were used for further experiments. The cells, after washing three times with pre-warmed HBSS, were equilibrated with 0.5 mL of HBSS in the apical chamber and 1.5 mL of HBSS in the basal chamber for 30 min at 37°C. Then the solution was withdrawn from the apical chamber and the FITC-insulin-loaded HA nanoparticles previously diluted in HBSS was added to the apical chamber. After the scheduled period of incubation at 5%  $\text{CO}_2$ , 95% humidity, and 37°C; solutions were then taken from basal chamber for further analysis by fluorescence spectrophotometer.

The apparent permeability coefficient ( $P_{\text{app}}$ ) and efflux ratio were calculated according to the following equations:

$$P_{\text{app}} = (d_Q/d_t) \times (1/AC_0) \quad (1)$$

$$\text{Efflux ratio} = P_{\text{app}}(\text{B to A})/P_{\text{app}}(\text{A to B}) \quad (2)$$

(17)

Where  $d_Q/d_t$  is the amount of insulin transported within a given period,  $A$  is the membrane surface area and  $C_0$  is the donor initial insulin concentration.  $P_{\text{app}}$  (A to B) and  $P_{\text{app}}$  (B to A) represent the apparent permeability coefficients in the basal-to-apical direction and the apical-to-basal direction, respectively.

### Fluorescence Microscope Visualization

For the observation of insulin-loaded HA nanoparticles across Caco-2 cell monolayer, cellular uptake was observed by fluorescence microscope. Caco-2 cells were seeded at a density of  $5 \times 10^4$  cells/ $\text{cm}^2$  into 24-well and incubated for 2 weeks to make sure tight junctions were formed. The freshly prepared FITC-insulin-loaded HA nanoparticles were diluted with HBSS at HA concentration of 100 and 200  $\mu\text{g/mL}$ . After rinsing each well with HBSS three times, the diluted samples were added (0.5 mL). After incubation for the schedule time, the wells were washed three times with ice-cold HBSS. Then

samples were observed by fluorescence microscope (IX 71, Olympus, Japan) with excitation and emission wavelengths of 490 and 525 nm, respectively.

### Permeation Measurements Across Excised Rat Small Intestine

*Ex vivo* absorption evaluation of FITC-insulin-loaded HA nanoparticles was carried out by permeation measurements in excised rat small intestine. Freshly excised rat duodenum, jejunum, and ileum tissue were washed with Krebs-Ringer buffer (KRB) and cut into pieces of about 5 cm each. One end of the excised tissue was tied up with a suture. HA nanoparticles containing 0.5 mg FITC-insulin were placed into the piece of tissue, followed by adding of 0.2 mL of Krebs-Ringer buffer and tying up the other end. The FITC-insulin solution at the same concentration was treated as the same procedure as control. The filled tissues were immersed in the vials filled with 10 mL of oxygenated Krebs-Ringer buffer, which was shaken gently (100 rpm) at 37°C. Sample solution (0.5 mL) was withdrawn from the serosal side at fixed time intervals and replaced with fresh buffer. Samples were assayed using fluorescence spectrophotometer with excitation wavelength of 490 nm and emission wavelength 525 nm.

### The Hypoglycemic Effect Following Oral Administration of Insulin-Loaded HA Nanoparticles

The experiment procedures involving animals and their care were conducted in conformity with NIH guidelines (NIH pub. no. 85-23, revised 1996) and were approved by Animal Care and Use Committee of Sun Yat-sen University (Guangzhou, China). Pharmacological effects of the insulin-loaded HA nanoparticles were determined by measuring the decrease of plasma glucose levels in diabetic rats. Sprague-Dawley male rats (200±20 g) were made diabetic prior to the study by intraperitoneal injection of 60 mg/kg streptozotocin in sodium citrate

buffer solution (pH 4.2). The rats were considered to be diabetic when the blood glucose  $\geq 16.7$  mmol/L. The diabetic rats were randomly divided into three groups (six rats in each group) for the hypoglycemic effect study. Group 1 was a control group which was treated with insulin solution (50 IU/kg) *via* a bulb tipped gavage needle. Group 2 was given insulin-loaded HA nanoparticles (50 IU/kg) orally. Group 3 was injected subcutaneously with insulin solution (1 IU/kg). Blood samples were collected from the tail vein every hour. Serum glucose level was assayed using a blood glucose meter (Roche, ACCU-CHEK, Advantage, Germany), and expressed as a percentage of the baseline serum glucose level.

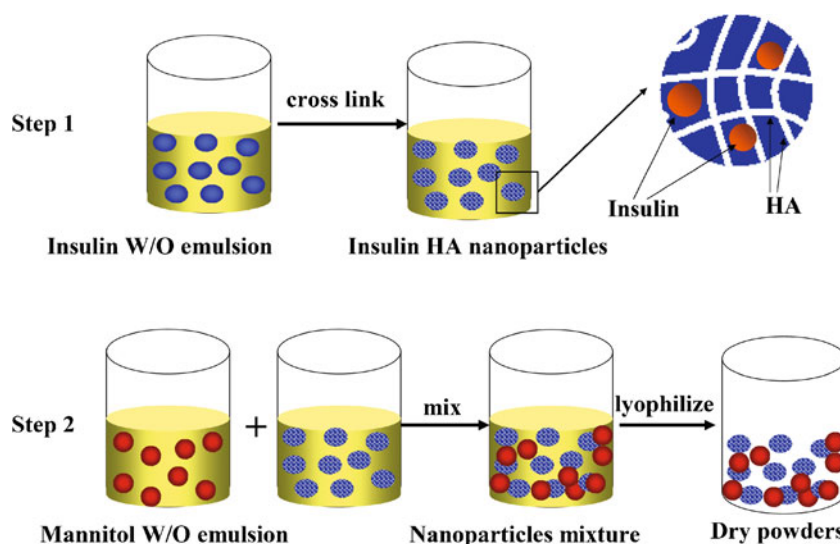
### Statistical Analysis

Data were expressed as the mean±the standard deviation. Statistical comparisons were performed using one-way analysis of variance (ANOVA, SPSS statistics 17.0). *p* values smaller than 0.05 or 0.01 indicated statistical significance.

## RESULTS AND DISCUSSION

### Preparation and Characterization of Insulin-Loaded HA Nanoparticles with High Entrapment Efficiency

In this study, we developed a novel reverse-emulsion-freeze-drying approach to prepare the HA nanoparticles with high insulin entrapment efficiency. The rationales of using HA nanoparticles for insulin oral delivery are: firstly, compared with the convenient approaches, the hydrophilic insulin entrapped in cross-linked HA nanoparticles was dispersed in oil continuous phase and not in water, resulting in more than 90% of insulin entrapment efficiency. Secondly polyanionic polysaccharide, HA, cannot open the tight junctions between contiguous epithelial cells as polycationic chitosan does, which suggest that HA is low toxicity to the intestinal epithelial cells and promises long-term safety for chronic insulin treatment.



**Scheme 1.** Preparation of insulin-loaded HA nanoparticles by the reverse-emulsion-freeze-drying (REFD) method

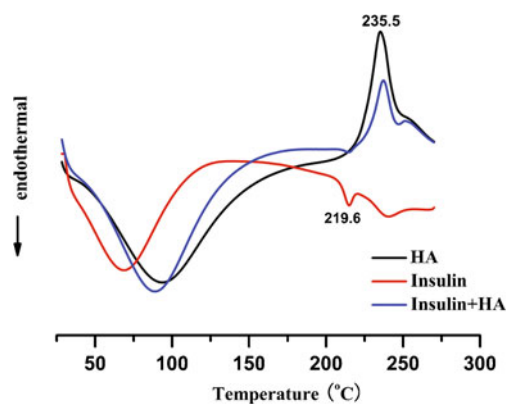


**Fig. 1.** DSC curves of HA, insulin, and mixture of HA and insulin

Thirdly, HA nanoparticles may increase cellular uptake of insulin in intestinal epithelial cells *via* HA-CD44 interaction. If HA could be used as both the matrix and ligand, HA nanoparticles would be low cost in comparison with either of the lectin or vitamin B<sub>12</sub> conjugated nanoparticles.

Insulin-loaded HA nanoparticles were prepared by a two-step process using the reverse-emulsion-freeze-drying (REFD) method, as shown in Scheme 1. First, the HA aqueous solution containing insulin and a small amount of ADH and EDC as cross-linkers was dispersed into nanodroplets in the nonpolar cyclohexane as external medium. In nanodroplets, EDC activated carboxyl groups of HA to form an amine-reactive HA intermediate (18). Then the activated HA intermediate was coupled with each other in the presence of ADH

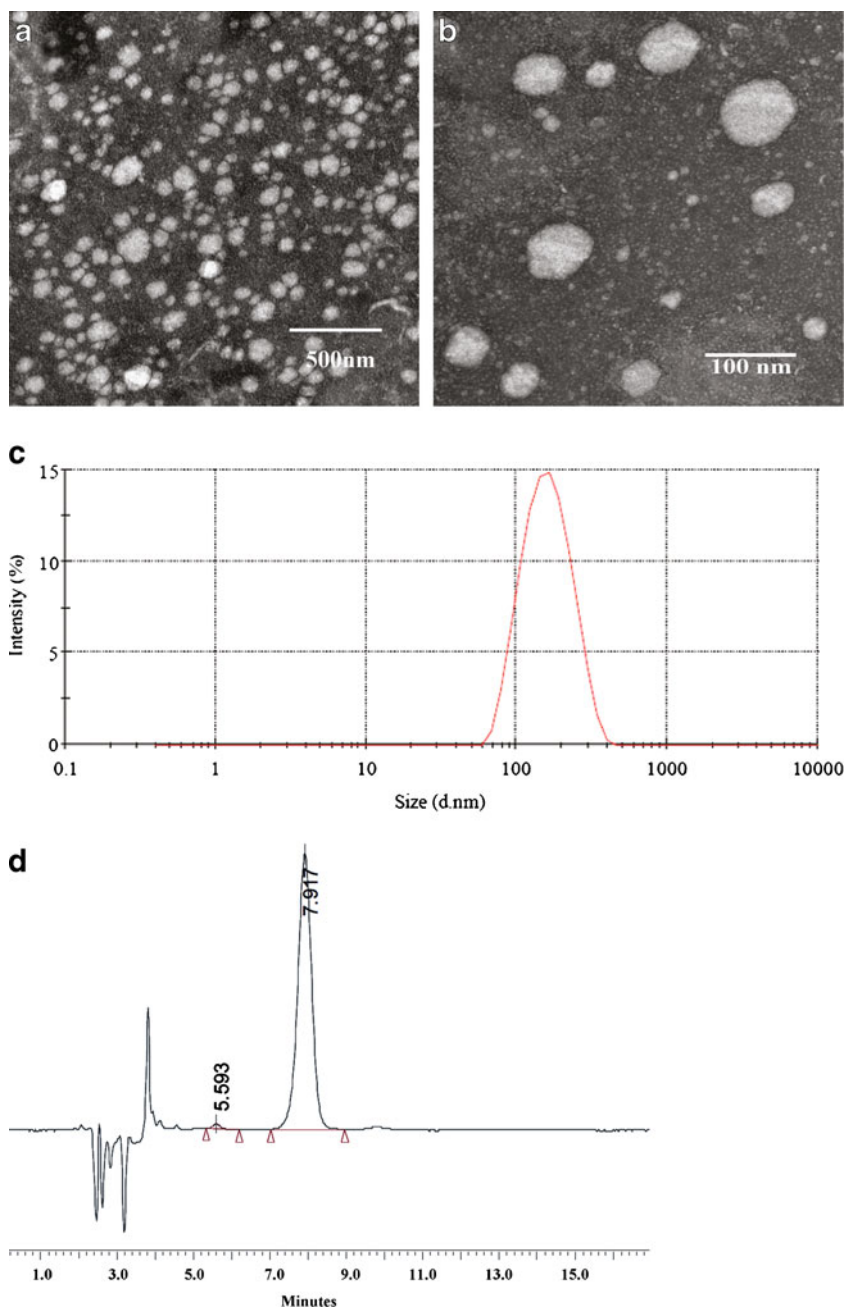


**Fig. 2.** **a, b** The TEM images and **c** size distribution of insulin-loaded HA nanoparticles. **d** The HPLC chromatogram of insulin diffused from the HA nanoparticles

**Table I.** Characterization of Insulin-Loaded HA Nanoparticles

Sample	Insulin HA-NPs
Particle size (nm)	182.2±7.53
Polydispersity index	0.163±0.01
Zeta potential (mV)	-42.13±1.44
Insulin entrapment efficiency (%)	94.79±4.97
Insulin-loading content (%)	18.95±1.00

All values are mean±S.D. ( $n=3$ )

to form the cross-linked HA nanoparticles containing insulin. In the second step, the saturated solution of mannitol with a high degree of dispersion in cyclohexane was mixed with insulin-loaded HA nanoparticles in cyclohexane. The mixture was lyophilized to collect the insulin-loaded HA nanoparticles dry powder. This REFD approach to prepare insulin-loaded nanoparticles had the outstanding advantages that the drug entrapment efficiency (~95%) and drug loading content were much higher as compared to the most widely investigated approaches such as ionic gelation method to prepare insulin-loaded chitosan–alginate nanoparticles and W/O/W emulsion method to prepare insulin-loaded PLGA nanoparticles (19). Insulin is a hydrophilic peptide hormone, while conventional preparation techniques for insulin nanoparticle formulations commonly used water as external phase and insulin tended to diffuse to the external phase, resulting in relatively low drug entrapment efficiency and drug loading content (20,21). Low drug entrapment efficiency is thought as one of the limitations for large-scale production. In the study, the REFD method could overcome the limitations of low entrapment efficiency and drug loading content of conventional insulin-loaded nanoparticles. Insulin was entrapped into hydrophilic HA nanoparticles as insulin is insoluble in the external phase, cyclohexane, resulting in its high drug entrapment efficiency. Furthermore, mannitol, one of the most commonly used excipients in the freeze-drying of macromolecules, in microdrops were extensively mixed with insulin-loaded HA nanoparticles before freeze-drying, which ensured quick and complete reconstitution of the lyophilized insulin-loaded HA nanoparticle powder in water. The oral acute toxicity of ADH as a cross-linker and cyclohexane as external media in this system are

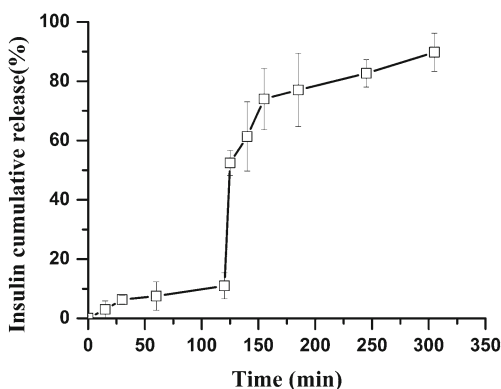


**Fig. 3.** *In vitro* release profiles of insulin from HA nanoparticles in the simulated gastric fluid (pH 1.2) and intestinal fluid (pH 6.8). Each value represents mean±S.D. ( $n=3$ )

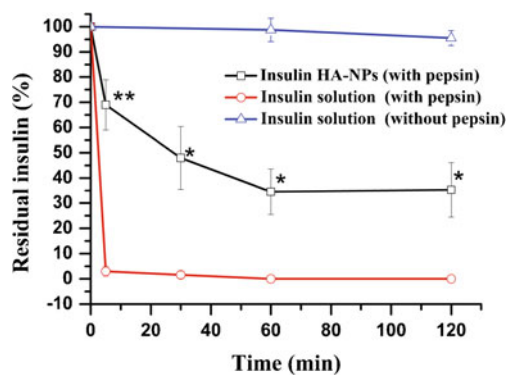


**Fig. 4.** Residual percentage of insulin after incubation of insulin solution (circle), insulin-loaded HA nanoparticles (square) in pepsin solution ( $n=3$ , mean±SD). Significant differences were marked with asterisks ( $*p<0.05$  and  $**p<0.01$ )

low and their LD50 in rats is greater than 5,000 mg/kg and 10,000 mg/kg, respectively (22,23). Furthermore, to ensure the complete reaction of all ADH and EDC, excess HA was used.

These HA nanoparticles with high insulin entrapment efficiency and loading content encouraged us to explore their properties as a drug carrier for insulin oral delivery. The interactions between hyaluronic acid and insulin were measured by DSC (Fig. 1). The peak at 219°C in the insulin curve represented roughly the beginning of decomposition. The peak at 235°C in HA curve was associated with thermal degradation. The DSC curve of HA and insulin mixture was similar to the overlap of HA and insulin curves. The results revealed that no obvious interaction between HA and insulin was observed. The HPLC chromatogram of insulin diffused from the HA nanoparticles showed except for solvent peaks only one peak was attributed to insulin in Fig. 2d. It suggested there was not any detectable degradation of insulin in these insulin nanoparticles. Insulin-loaded HA nanoparticles with  $-42.1\pm 1.4$  mV of surface charges and around  $182.2\pm 7.5$  nm of particle size was prepared into lyophilized powder (Table I). The spherical and well-defined insulin-loaded HA nanoparticles, as shown in Fig. 2a, b, with averaged 94.8% of drug entrapment efficiency and 19.0% of drug loading content was used to further experiments.

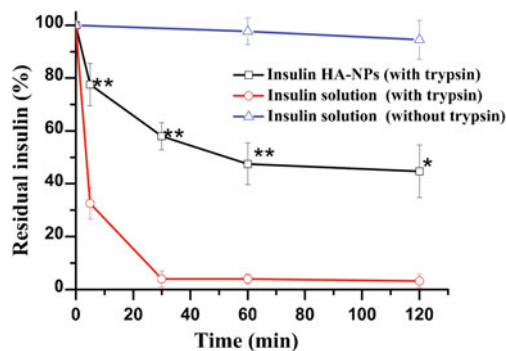


**Fig. 5.** Residual percentage of insulin after incubation of insulin solution (circle), insulin-loaded HA nanoparticles (square) in trypsin solution ( $n=3$ ; mean±SD). Significant differences were marked with asterisks ( $*p<0.05$  and  $**p<0.01$ )

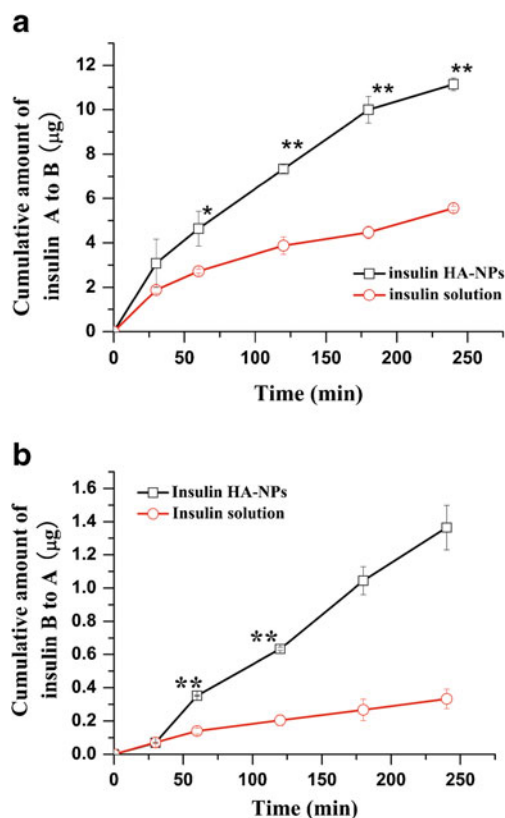


**Fig. 6.** Cumulative amount of FITC-insulin transported across Caco-2 cell monolayers **a** from apical chamber to basolateral chamber and **b** from basolateral chamber to apical chamber. Each value represents mean±S.D. ( $n=3$ ). Significant differences were marked with asterisks (\* $p<0.05$  and \*\* $p<0.01$ )

### In Vitro Insulin Released from pH-Sensitive HA Nanoparticles

Polymeric nanoparticles for controlled release of insulin are thought as one of effective ways to enhance its oral absorption (24). Figure 3 illustrated the release profile of insulin from HA nanoparticles in SGF (pH 1.2) during the first 120 min and then in SIF (pH 6.8) for another 180 min. Results showed that the cumulative insulin released from HA nanoparticles in SGF under sink conditions was less than 10%. In contrast, more than 80% of insulin was released from HA nanoparticles in SIF within 60 min. These results suggest that the HA nanoparticles were pH sensitive because the pH of the release medium governed the entrapped insulin release. HA, a weak acid, has an intrinsic pKa value of about 3.0, therefore, a change in pH affects the extent of ionization of HA chains (25). The release rate of insulin from HA nanoparticles in

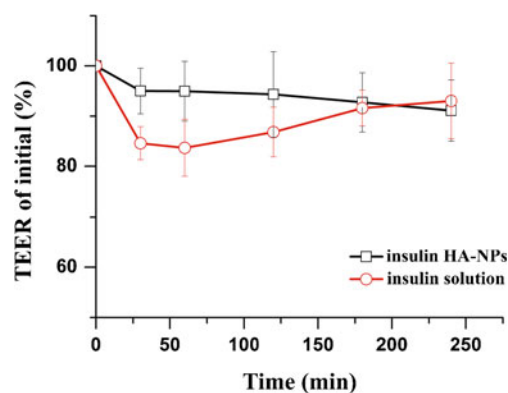


**Fig. 7.** TEER values were monitored as a function of time evaluated during permeability experiments from apical chamber to basolateral chamber with the Caco-2 cells seeded on 12-well transwell plates. Insulin solution (circle), insulin-loaded HA nanoparticles (square) ( $n=3$ ; mean±SD)

SGF was slow mostly due to a very low degree of ionization of HA at pH 1.2. The pH-sensitive HA nanoparticles could protect insulin against a strong-acidic gastric environment, and deliver the intact insulin to the small intestine.

### HA Nanoparticles Protecting Insulin Against Enzymatic Degradation

The physiological activity of insulin is destroyed by protease enzymes in GI tract, which is one of barriers to oral insulin delivery (10). To investigate the effect of HA nanoparticles on protecting insulin against enzymatic degradation, the enzymatic digestion assay was performed. Pepsin and trypsin, two of three principal proteolytic enzymes in the digestive system, were chosen to digest insulin. It was noted that the biodegradation degree of insulin loaded in HA nanoparticles was obviously less than that of insulin solution, as shown in Figs. 4 and 5.  $31.01\pm 9.95\%$  and  $27.51\pm 8.03\%$  of insulin entrapped in HA nanoparticles degraded at the initial stage of pepsin and trypsin digestion, respectively, while  $97.02\pm 5.30\%$  and  $62.50\pm 5.94\%$  of insulin solution disappeared under the same conditions. Furthermore,  $35.27\pm 10.83\%$  and  $44.69\pm 9.98\%$  of insulin entrapped in HA nanoparticles remained intact after 2 h of pepsin and trypsin digestion, respectively. In contrast, correspondingly, no intact insulin and  $3.14\pm 2.55\%$  of intact insulin in solution could be detected. These results confirmed earlier studies HA nanoparticles could protect insulin against protease enzymes to a certain extent in GI tract as others polymeric nanoparticles did (26). It was likely attributed to the entrapment of insulin in nanoparticles and then shielding it from enzyme digestion.

**Table II.** The Apparent Permeability Coefficient and Efflux Ratio for Caco-2 Cells

Samples	$P_{app}\times 10^{-7}(\text{cm s}^{-1})$		$P_{app(B\ to\ A)}/P_{app(A\ to\ B)}$
	$P_{app(A\ to\ B)}$	$P_{app(B\ to\ A)}$	
Insulin HA-NPs	$27.45\pm 1.05^*$	$3.34\pm 0.32$	$0.12\pm 0.016$
Insulin solution	$13.69\pm 0.33$	$0.82\pm 0.13$	$0.06\pm 0.011$

Each value represents mean±S.D. ( $n=3$ )

\* $p<0.05$

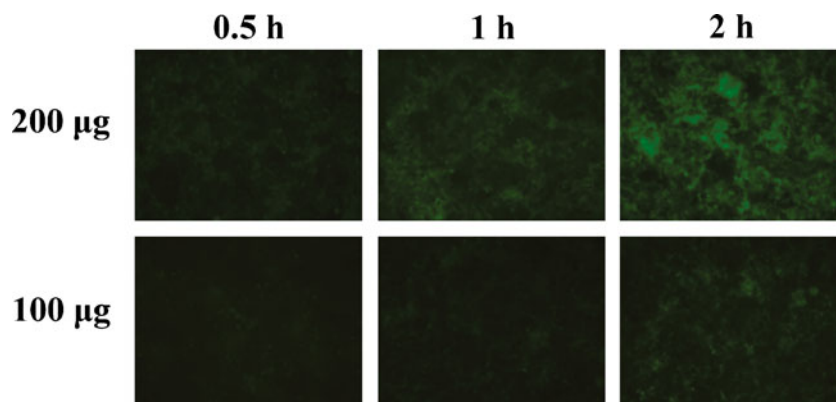


**Fig. 8.** Fluorescent microscopy images of Caco-2 cells exposed to 100 and 200 µg of FITC-insulin-loaded HA nanoparticles for 0.5, 1 and 2 h at 37°C

### Transepithelial Transport of HA Nanoparticles Across Caco-2 Cell Monolayer

In order to evaluate the intestinal transepithelial transport and predict insulin absorption across the human intestine *in vitro*, the permeability of insulin-loaded HA nanoparticles across Caco-2 cell monolayer from apical chamber to basolateral chamber was measured, as shown in Fig. 6a. The insulin encapsulated within HA nanoparticles was more efficiently transported in comparison with insulin solution, at the same concentration. For insulin-loaded HA nanoparticles, their permeated amounts of transported insulin exceeded that of insulin solution at each time point. The amounts of entrapped insulin in HA nanoparticles across Caco-2 cell monolayer were roughly three times more than that of insulin solution after 4-h incubation. Furthermore, as the apparent permeability coefficients ( $P_{app}$  (A to B)) obtained from Caco-2 cell transport studies are reported to correlate to human intestinal absorption (27), the  $P_{app}$  (A to B) of samples was calculated (Table II) and demonstrated that the  $P_{app}$  (A to B) of insulin entrapped in HA nanoparticles showed statistically significant ( $p < 0.05$ ) more than twofold increase in comparison with that of insulin solution. It is well-known that multiple efflux transporters such as P-glycoprotein are identified in Caco-2 cells and responsible for restricting intestine absorptions for their substrates (28). The efflux ratio of  $P_{app}$  (B–A) to  $P_{app}$  (A–B)

was calculated as 0.12, which was less than 1, suggesting that the HA nanoparticle-mediated transport of insulin across Caco-2 cell monolayers was *via* active transport.

### HA Nanoparticles Delivering Insulin Via Transcellular Pathway

To speculate whether the HA nanoparticles delivered insulin *via* the transcellular or paracellular pathway, transendothelial electrical resistance (TEER) was measured to estimate the integrity of the Caco-2 cell monolayer treated with insulin samples. The Caco-2 cell monolayer after exposure to insulin-loaded HA nanoparticles for 4 h did not show any significant change in TEER. The TEER values were decreased by less than 10% (Fig. 7). Normal differentiated polarized Caco-2 cells have tight junctions with a TEER above 200  $\Omega\text{cm}^2$ , consequently a TEER value above 200  $\Omega\text{cm}^2$  indicated the integrity of the Caco-2 cell monolayer (29). In this study, all the TEER values of HA nanoparticle samples were greater than 390  $\Omega\text{cm}^2$  during the incubation period. This demonstrated that HA nanoparticles did not open the tight junctions of Caco-2 cell monolayer to allow the transport of insulin along the paracellular pathway. Although the paracellular pathway by opening of the epithelial tight junctions is thought as one of the most efficient way to orally

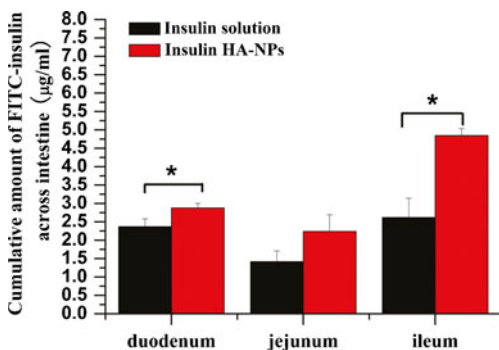


**Fig. 9.** Cumulative amount of FITC-insulin transported across intestinal walls. Freshly isolated rat duodenum, jejunum, and ileum were filled with FITC-insulin solution, FITC-insulin-loaded HA nanoparticles, and 1 mL samples were withdrawn from outside the tissues. The samples were analyzed by fluorescence spectrophotometer. \* $p < 0.05$ . Each value represents mean  $\pm$  S.D. ( $n = 3$ )

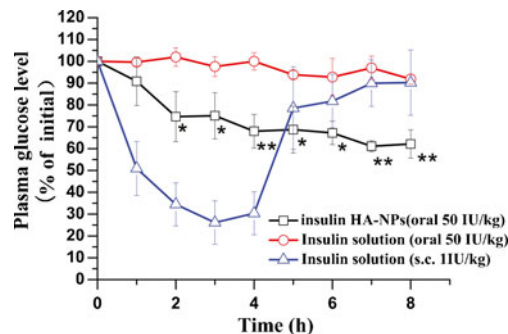


**Fig. 10.** Changes in blood glucose level *versus* time profiles following oral administration of 50 IU/kg insulin solution (circle), 50 IU/kg insulin-loaded HA nanoparticles (square) and 1 IU/kg insulin solution s.c. (triangle) to STZ-induced diabetic rats. Insulin-loaded HA nanoparticles showed statistically significant difference in hypoglycemic effect compared with insulin solution (\* $p < 0.05$ ; \*\* $p < 0.01$ ). Each value represents mean  $\pm$  S.D. ( $n = 6$ )



deliver peptides by polymeric nanoparticles as cationic chitosan nanoparticles did in earlier studies (30), the safety of opening tight junctions for chronic drug therapy has yet to be demonstrated (11). Furthermore, cellular uptake of FITC-insulin-loaded HA nanoparticles by Caco-2 cells was observed by fluorescence microscopy. The fluorescent images as shown in Fig. 8, 200  $\mu\text{g}$  of insulin-loaded nanoparticles showed significantly more green fluorescent signals in Caco-2 cells than 100  $\mu\text{g}$  of insulin formulations. The cellular uptake of insulin-loaded HA nanoparticles also increased with incubation time, reaching a steady state at 2 h. The cellular uptake indicated that the Caco-2 cell uptake of insulin-loaded HA nanoparticles depended upon the concentration of nanoparticles and the time of incubation. These results also confirmed that the anionic HA nanoparticles carrying insulin were transported across Caco-2 cell monolayer *via* transcellular pathway.

### **Ex Vivo Insulin-Loaded HA Nanoparticles Across Excised Rat Small Intestine**

The enhancement of insulin transport across Caco-2 cell monolayers by HA nanoparticles encouraged us to further investigate its absorption behavior in an animal model. First, the permeability of insulin-loaded HA nanoparticles through rat small intestine containing mucosa was evaluated *ex vivo* as shown in Fig. 9. The small intestine is divided into three sections: duodenum, jejunum, and ileum. The transport studies of insulin-loaded HA nanoparticles across freshly excised three segments of rat small intestines showed the following ranking: ileum > duodenum > jejunum. Furthermore, the amounts of transported insulin by HA nanoparticles across the ileum and duodenum were significantly greater than that of insulin solution. The results suggested that HA nanoparticles could improve transport of insulin across excised rat small intestine containing mucosa and enterocytes.

### **In Vivo Assessment of the Oral Activity of Insulin-Loaded HA Nanoparticles**

HA nanoparticles as oral insulin delivery system were assessed by measuring blood glucose levels in rats with streptozotocin-induced diabetes. The hypoglycemic profiles showed the diabetic rats receiving oral treatment with 50 IU/kg of insulin-loaded HA nanoparticles induced decrease in blood glucose level of 24% in 2 h and 32–39% in during 3–8 h, as shown in Fig. 10. Conversely, the group treated with the same dose of insulin solution showed no change in blood glucose level during the experimental period. Compared with oral insulin solution-treated diabetic rats, the blood glucose levels were statistically significant decreased in the diabetic group treated with insulin-loaded HA nanoparticles ( $p < 0.05$ ). However, the diabetic rats injected subcutaneously with insulin solution still showed a much stronger hypoglycemic effect after treatment in 4 h compared with the group with oral treatment of insulin-loaded HA nanoparticles. These results demonstrated that the insulin-loaded HA nanoparticles possessed stronger oral antidiabetic activities than insulin solution, and yet its hypoglycemic effect was still not comparable to that of insulin injections.

## **CONCLUSIONS**

The present study developed novel insulin-loaded HA nanoparticles which showed great potential for oral insulin delivery. The insulin-loaded HA nanoparticles were prepared by REFD method with average size of 182.2 nm and high entrapment efficiencies (approximately 95%). The pH-sensitive HA nanoparticles as an oral delivery carrier had advantages in protecting insulin against the strongly acidic environment of the stomach, and not destroying the junction integrity of epithelial cells which promise long-term safety for chronic drug therapy. HA nanoparticles delivered insulin across Caco-2 cell monolayers mainly *via* transcellular pathway. The  $P_{\text{app}}$  (A–B) of HA nanoparticle-mediated system had more than twofold increase compared with insulin solution, which has been shown to correlate to human intestinal absorption. The results of permeability through the excised rat small intestine confirmed that HA nanoparticles significantly enhanced insulin transport through the duodenum and ileum. The diabetic rats treated with oral insulin-loaded HA nanoparticles also showed stronger hypoglycemic effects than insulin solution. Therefore, these HA nanoparticles would be a promising candidate for oral insulin delivery.

## **ACKNOWLEDGMENT**

The authors gratefully acknowledge the Fundamental Research Funds for the Central Universities (project no. 09ykpy67) for their financial support of this research.

## **REFERENCES**

1. Khafagy E, Morishita M, Onuki Y, Takayama K. Current challenges in non-invasive insulin delivery systems: a comparative review. *Adv Drug Deliv Rev.* 2007;59(15):1521–46.
2. Iyer H, Khedkar A, Verma M. Oral insulin—a review of current status. *Diabetes Obes Metab.* 2010;12(3):179–85.
3. Sarmento B, Ribeiro A, Veiga F, Sampaio P, Neufeld R, Ferreira D. Alginate/chitosan nanoparticles are effective for oral insulin delivery. *Pharm Res.* 2007;24(12):2198–206.
4. Santander-Ortega MJ, Bastos-Gonzalez D, Ortega-Vinuesa JL, Alonso MJ. Insulin-loaded PLGA nanoparticles for oral administration: an *in vitro* physico-chemical characterization. *J Biomed Nanotechnol.* 2009;5(1):45–53.
5. Almeida AJ, Souto E. Solid lipid nanoparticles as a drug delivery system for peptides and proteins. *Adv Drug Deliv Rev.* 2007;59(6):478–90.
6. Wang JJ, Zeng ZW, Xiao RZ, Xie T, Zhou GL, Zhan XR, *et al.* Recent advances of chitosan nanoparticles as drug carriers. *Int J Nanomedicine.* 2011;6:765–74.
7. Zhang N, Ping Q, Huang G, Xu W, Cheng Y, Han X. Lectin-modified solid lipid nanoparticles as carriers for oral administration of insulin. *Int J Pharm.* 2006;327(1–2):153–9.
8. Chalasani KB, Russell-Jones GJ, Yandrapu SK, Diwan PV, Jain SK. A novel vitamin B12-nanosphere conjugate carrier system for peroral delivery of insulin. *J Control Release.* 2007;117(3):421–9.
9. Zhang N, Li J, Jiang W, Ren C, Li J, Xin J, *et al.* Effective protection and controlled release of insulin by cationic beta-cyclodextrin polymers from alginate/chitosan nanoparticles. *Int J Pharm.* 2010;393(1–2):212–8.
10. Woitiski CB, Carvalho RA, Ribeiro AJ, Neufeld RJ, Veiga F. Strategies toward the improved oral delivery of insulin nanoparticles via gastrointestinal uptake and translocation. *BioDrugs.* 2008;22(4):223–7.
11. Chen MC, Sonaje K, Chen KJ, Sung HW. A review of the prospects for polymeric nanoparticle platforms in oral insulin delivery. *Biomaterials.* 2011;32(36):9826–38.

12. Li SD, Huang L. Pharmacokinetics and biodistribution of nanoparticles. *Mol Pharm*. 2008;5(4):496–504.
13. Bodnár M, Daróczy L, Batta G, Bakó J, Hartmann JF, Borbély J. Preparation and characterization of cross-linked hyaluronan nanoparticles. *Colloid Polym Sci*. 2009;287:991–1000.
14. Necas J, Bartosikova L, Brauner P, Kolar J. Hyaluronic acid (hyaluronan): a review. *Vet Med*. 2008;53(8):397–411.
15. Kogan G, Soltés L, Stern R, Gemeiner P. Hyaluronic acid: a natural biopolymer with a broad range of biomedical and industrial applications. *Biotechnol Lett*. 2007;29(1):17–25.
16. Holmes K, Lantz LM, Fowlkes BJ, Schmid I, Giorgi JV. Preparation of cells and reagents for flow cytometry. In: Coligan JE, Kruisbeek AM, Margulles DH, Shevac EM, Strober W, editors. *Current protocols in immunology*. New York: Wiley; 2000.
17. Huang L, Berry L, Ganga S, Janosky B, Chen A, Roberts J, *et al*. Relationship between passive permeability, efflux, and predictability of clearance from *in vitro* metabolic intrinsic clearance. *Drug Metab Dispos*. 2010;38(2):223–31.
18. Luo Y, Kirker KR, Prestwich GD. Cross-linked hyaluronic acid hydrogel films: new biomaterials for drug delivery. *J Control Release*. 2000;69(1):169–84.
19. Xie SY, Wang SL, Zhao BK, Han C, Wang M, Zhou WZ. Effect of PLGA as a polymeric emulsifier on preparation of hydrophilic protein-loaded solid lipid nanoparticles. *Coll Surf B: Biointer*. 2008;67(2):199–204.
20. Cui FD, Tao AJ, Cun DM, Zhang LQ, Shi K. Preparation of insulin loaded PLGA-Hp55 nanoparticles for oral delivery. *J Pharm Sci*. 2007;96(2):421–7.
21. Zhang Y, Wei W, Lv P, Wang L, Ma G. Preparation and evaluation of alginate-chitosan microspheres for oral delivery of insulin. *Eur J Pharm Biopharm*. 2011;77(1):11–9.
22. Liebert MA. Final report on the safety assessment of adipic acid dihydrazide. *J Am Coll Toxicol*. 1994;13(3):154–6.
23. Kimura ET, Ebert DM, Dodge PW. Acute toxicity and limits of solvent residue for sixteen organic solvents. *Toxicol Appl Pharmacol*. 1971;19(4):699–704.
24. Damgé C, Maincent P, Ubrich N. Oral delivery of insulin associated to polymeric nanoparticles in diabetic rats. *J Control Release*. 2007;117(2):163–70.
25. Brown MB, Jones SA. Hyaluronic acid: a unique topical vehicle for the localized delivery of drugs to the skin. *J Eur Acad Dermatol Venereol*. 2005;19(3):308–18.
26. Ramesan RM, Sharma CP. Challenges and advances in nanoparticle-based oral insulin delivery. *Expert Rev Med Devices*. 2009;6(6):665–76.
27. Walgren RA, Walle UK, Walle T. Transport of quercetin and its glucosides across human intestinal epithelial Caco-2 cells. *Biochem Pharmacol*. 1998;55(10):1721–7.
28. Lai Y, Chiang PC, Blom JD, Li N. Comparison of *in vitro* nanoparticles uptake in various cell lines and *in vivo* pulmonary cellular transport in intratracheally dosed rat model. *Nanoscale Res Lett*. 2008;3(9):321–9.
29. MacCallum A, Hardy SP, Everest PH. *Campylobacter jejuni* inhibits the absorptive transport functions of Caco-2 cells and disrupts cellular tight junctions. *Microbiology*. 2005;151(Pt 7):2451–8.
30. Nagpal K, Singh SK, Mishra DN. Chitosan nanoparticles: a promising system in novel drug delivery. *Chem Pharm Bull(Tokyo)*. 2010;58(11):1423–30.